Malaysian Journal of Analytical Sciences (MJAS)
Published by Malaysian Analytical Sciences Society

STRUCTURAL AND ELECTROCHEMICAL CHARACTERISATIONS OF LANTHANUM-BASED COBALT FERRITE AND BARIUM CERATE-ZIRCONATE OXIDES AS COMPOSITE CATHODE FOR PROTON CERAMIC FUEL CELL

(Pencirian Struktur dan Elektrokimia Lantanum Berasaskan Kobalt Ferum Oksida dan Barium Serat-Zirkonat Oksida Sebagai Komposit Katod untuk Aplikasi Sel Fuel Seramik Proton)

Nurul Izzati Abd Malek[1], Ismariza Ismail[2], Abdul Mutalib Md Jani[3], Mohd Hafiz Dzarfan Othman[4], Nafisah Osman[1,5]*

[1]Proton Conducting Fuel Cell Research Group, Faculty of Applied Sciences, Universiti Teknologi MARA, 40450 Shah Alam, Selangor, Malaysia
[2]Faculty of Engineering Technology, Universiti Malaysia Perlis, 02100 Padang Besar, Perlis, Malaysia
[3]Faculty of Applied Sciences, Universiti Teknologi MARA, 35400 Tapah Road, Tapah, Perak, Malaysia
[4]Advanced Membrane Technology Research Centre (AMTEC), School of Chemical & Energy Engineering, Faculty of Engineering, Universiti Teknologi Malaysia, 81310 UTM Skudai, Johor, Malaysia
[5]Faculty of Applied Sciences, Universiti Teknologi MARA Perlis, 02600 Arau, Perlis, Malaysia

[*]Corresponding author: fisha@uitm.edu.my

Received: 12 September 2021; Accepted: 12 July 2022; Published: 25 August 2022

Abstract

This study investigated the composite cathode of $LaSrCoFeO_3$-$BaCeZrYO_3$ (LSCF-BCZY) in a ratio of 7 : 3. A 13-mm symmetrical half-cell was fabricated using the dry pressing and spin-coating techniques to yield the configuration of LSCF-BCZY|BCZY|LSCF-BCZY. The phase of the sample was verified using the X-Ray Diffraction (XRD) spectroscopy. The electrochemical and microstructure of the half-cell were characterized using the Electrochemical Impedance Spectroscopy and Scanning Electron Microscopy (SEM), respectively. The XRD analysis showed that the single-phase structure of LSCF and BCZY was still preserved at the calcination temperature of 900 ºC. The half-cell demonstrated a thermally activated trend in a humidified atmosphere with area-specific resistance values of 0.25, 0.33, 1.02, 1.64, and 5.75 Ω.cm^2 at temperatures of 800, 750, 700, 650, and 600 ºC, respectively. The SEM image revealed that the 10-µm LSCF-BCZY layer was well-adhered on the dense BCZY electrolyte surface. This synthesised LSCF-BCZY in the ratio of 7 : 3 demonstrated excellent characteristics as a composite cathode for PCFCs.

Keywords: composite cathode, single phase, spin coating, proton ceramic fuel cells

Abstrak

Dalam kajian ini, komposit katod daripada $LaSrCoFeO_3$-$BaCeZrYO_3$ (LSCF-BCZY) dengan nisbah 7 : 3 dipilih disebabkan kelebihanya berbanding dengan LSCF tulen. Teknik penekanan kering dan saduran berpusing telah digunakan untuk menghasilkan 13-mm sel separa simetri dengan konfigurasi iaitu LSCF-BCZY|BCZY|LSCF-BCZY. Pembentukan fasa sampel telah disahkan oleh pembelauan sinar-X (XRD). Sifat elektrokimia dan struktur mikro daripada sel separa simetri masing-masing telah diciri menggunakan spektroskopi impedans elektrokimia (EIS) dan pengimbasan mikroskop elektron (SEM). Pada suhu kalsinan 900 ^oC, komponen LSCF dan BCZY tidak menunjukkan sebarang perubahan dan berfasa tunggal seperti dibuktikan melalui analisis XRD. Sel ini menunjukkan kecenderungan aktif secara terma, yang disahkan melalui pengukuran EIS dalam atmosfera lembap dengan kawasan rintangan khusus (ASR) masing-masing iaitu 0.25, 0.33, 1.02 , 1.64, dan 5.75 $\Omega.cm^2$ pada suhu 800, 750, 700, 650 dan 600 ^oC. Gambar SEM menunjukkan bahawa lapisan 10 μm LSCF-BCZY melekat dengan baik pada permukaan elektrolit padat BCZY. Maka, penghasilan LSCF-BCZY dengan nisbah 7 : 3 menunjukkan ciri-ciri yang terbaik sebagai katod komposit bagi aplikasi PCFC.

Kata kunci: katod komposit, fasa tunggal, saduran berpusing, sistem sel fuel seramik proton

Introduction

A Proton Ceramic Fuel Cell (PCFC) is a green device that converts chemical energy to electrical energy with heat and water as by-products for a high-power generation system. However, a high cathode polarisation resistance (R_p) reduces the overall cell system performance substantially, particularly at the intermediate temperature range of 500 to 800 ^oC [1]. The rising trend in R_p is related to the lack of a surface-active site for the oxygen reduction process (ORR) at the triple-phase boundary (TPB) that connects the electrolyte, cathode, and gas phase. Thus, selecting the best materials for the cathode component is crucial for the PCFC system because materials will exhibit different characteristics when coupled with other materials or operating at elevated temperatures. In this respect, pure $LaSrCoFeO_3$ (LSCF) is a well-known cathode material for PCFCs because it contains more excellent ionic and electronic charge carrier species than traditional cathodes [2]. However, because LSCF has a limited number of TPB sites, various methods or materials have been suggested to increase the TPB length [3, 4]. One of the suggested methods is the use of a composite cathode for integrating proton conductors, mixed electronic-ionic conductors, or a catalytic layer [5].

For PCFCs, a composite cathode is produced by mixing materials of the cathode and proton conductor electrolyte for high-kinetic ORR. The electrical conductivity of the composite cathode increased about two times higher than the pure cathode [6 - 8]. However, an excessive amount (> 50%) of protonic species in the mixed ionic-electronic conductor MIEC cathodes caused water loading across the bulk cathode, reducing the overall performance of the fuel cell [9, 10]. Meanwhile, protonic species based on cerate-zirconate oxides exhibited high conductivity; they were chemically stable and compatible with LSCF cathodes [11]. Recently, adding some protonic species, for example, doped-barium cerate zirconate oxide, into the LSCF cathode using chemical approaches lengthened the TPB [12].

In general, a symmetrical half-cell is fabricated for electrochemical studies to evaluate the behaviour of the composite cathode. The half-cell requires the optimised electrolyte substrate and cathode thin-film design. The electrolyte substrate is dry-pressed at the desired pressure and sintered at high temperatures to obtain the dense pellet. The cell is subjected to electrochemical impedance spectroscopy (EIS) measurement to study the material behaviour and performance. A suitable equivalent circuit for EIS spectra is introduced to fit the EIS spectrum via a fitting procedure. Information or data gained is used to calculate capacitance, arc summit frequency, and area-specific resistance (ASR) of the half-cell as a function of temperature. The Adler Lane Steel (ALS) model is used to extract the associated response in the EIS spectrum.

In this study, $BaCeZrYO_3$(BCZY) was chosen as a proton-conducting medium to form the composite cathode of LSCF-BCZY. The structural and electrochemical properties of the prepared cathode were further analysed and characterised.

Materials and Methods

The $LaSrCoFeO_3$ cathode powder was produced using a modified sol-gel process in which all the metal nitrate salts in the universal solvent were dissolved, followed by adding citric acid and ethylenediaminetetraacetic acid (EDTA). Upon alkalinising the mixture to pH 9 with ammonium hydroxide, ethylene glycol was added, and the brownish gel produced was calcined for five hours at 900 ºC. The single-phased BCZY powder and the high relative density pellet (97.1%) were prepared as previously described [13]. The LSCF and BCZY powders were mixed in the ratio of 7: 3 weight percent (wt%) to form the LSCF-BCZY composite cathode. The composite powder was transformed into cathode slurry and spin-coated on both sites of the BCZY pellet under optimised conditions (2,000 rpm for 30 s). The half-cell with the configuration of LSCF-BCZY|BCZY|LSCF-BCZY was sintered at 600 ºC for one hour and 900 ºC for three hours.

The prepared powder and half-cell were characterised using X-ray diffraction (XRD) spectroscopy, EIS, and scanning electron microscopy (SEM). For XRD, the LSCF-BCZY powder was radiated with Cu-K_α at the ambient temperature at the wavelength of 1.5406 Å using 8.04 keV (PANalytical X'Pert PRO MRD PW 3040). The scanning was set at the rate of 0.02 s^{-1} to collect the two thetas from 20º to 80º. The XRD data was analyzed with X'Pert HighScore Plus software (version 5.1, Malvern Panalytical) and compared to the Joint Committee on Powder Diffraction Standard (JCPDS) card number 089-1268 for LCSF and 01-089-2485 for BCZY. The perovskite phases were calculated using the Swarts and Shrout equation. Meanwhile, the symmetrical half-cell was passed through wet air at the flow rate of 90 mL/min, and the electrochemical parameter was measured between 1 MHz and 10 MHz with amplitude voltages ranging from 3 to 5 mV at 600 – 800 ºC using the electrochemical workstation ZIVE SP2 (ZIVE LAB WonATech). An equivalent circuit of L_s-R_s(R1Q1)-(R2Q2) was used for the impedance spectrum analysis using the test station (ZIVE ZMAN™ 2.4). Values of capacitance, arc summit frequency, and polarisation resistance were calculated for each temperature using the equations reported in another study [14]. The raw and fitted data were re-plotted using the software Origin 2019b. After electrochemical testing, the morphology of pellets was evaluated using SEM with energy dispersive X-ray (EDX). The software ImageJ was used to measure the porosity of the SEM image.

Results and Discussion

Figure 1 shows the XRD pattern of LSCF-BCZY composite cathode powder upon calcination at 900 ºC. All diffraction peaks agreed with JCPDS-card no. (LSCF ID: 01-089-1268) and (BCZY ID: 01-089-2485) with orthorhombic and cubic structures, respectively. More than 90% of the single perovskite phase was formed for both LSCF and BCZY, indicating that these materials maintained their phases after the heat treatment at 900 °C. The prominent peaks were indexed using Miller Indices (hkl) reflected plane as follows: (110), (020), (202), (220), (132), (224), and (332) for LSCF, and (110), (200), (211), (220), and (222) for BCZY. The lattice constants of LSCF and BCZY were calculated using the software Mathcad 14.0 (Mathsoft). Table 1 shows the lattice constants of LSCF and BCZY, and they agreed with the reference data. These values were consistent with the finding of another study [15] for LSCF-BCZY treated at 1,000 ºC.

Figure 2 shows the Nyquist impedance plot of the fabricated half-cell in humidified air at temperatures ranging from 600 to 800 ºC. As the temperature increased, the impedance spectrum became smaller in size, obeying the thermally activated behaviour, as expected by Arrhenius's Law [16]. The arcs were resolved using an equivalent circuit (the inset of Figure 2). The first arc, represented by R_1Q_1, was referred to as an electronic charge transfer that occurred at the cathode surface. The second arc, R_2Q_2, was associated with the ionic charge transfer reaction at the cathode-electrolyte interphase. The calculated capacitance ranged from 10^{-2} - 10^{-4} for the R_1Q_1 circuit and 4 x 10^{-5} - 10^{-7} for the R_2Q_2 circuit [5], denoting the respective cathode process. Also, the arc summit frequency confirmed the presence of these two arcs in the middle and low-frequency regions. ASR values of 0.25, 0.33, 1.02, 1.64, and 5.75 Ω.cm^2 were obtained between 800 and 600 ºC at intervals of 50 ºC. ASR values of the pure LSCF increased by about one time

higher than modified samples (800 – 600 ºC: 1.06, 1.13, 3.13, and 6.50 Ω.cm^2). Compared to the pure LSCF, the reduction of ASR values for LSCF-BCZY suggested that the use of composite cathode could potentially enhance the performance of PCFC.

Figure 3 shows the SEM images of the fractured cross-section and cathode surface of the LSCF-BCZY|BCZY|LSCF-BCZY symmetrical half-cell after the electrochemical measurement. There was no sign of crack and delamination in the cell, indicating a good adhesion between a 10-µm LSCF layer and a dense electrolyte that promoted a low contact resistance [15]. The cathode surface showed a well dispersed and homogenised microstructure with a porosity of 32%. This amount was sufficient to allow better oxygen diffusion through the cathode material as the required porosity ranged from 20% to 40% [16]. Good adhesion between LSCF-BCZY cathode and BCZY electrolyte as well as the homogenised microstructure of the LSCF layer reduced the resistance of cathode bulk, leading to fast surface oxygen ion diffusion [5, 17].

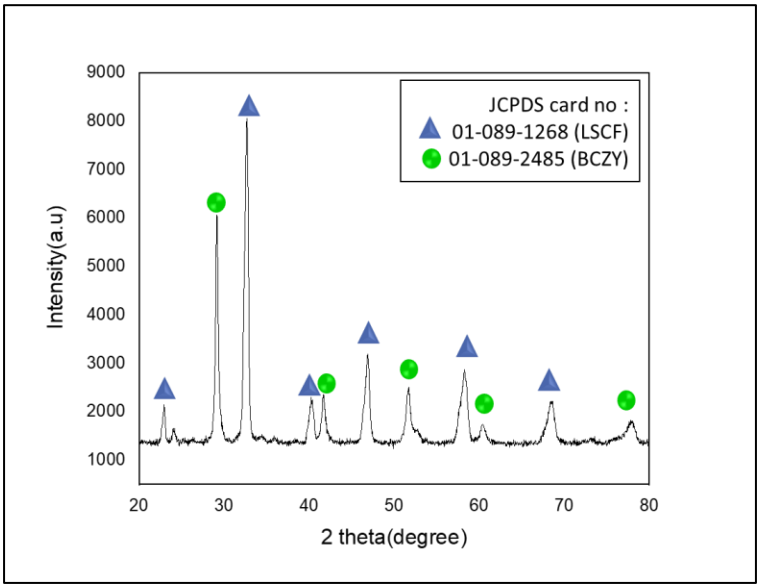

Figure 1. XRD pattern of the LSCF-BCZY composite cathode after calcined at T = 900ºC.

Table 1. Lattice parameter of the LSCF and BCZY taken from JCPDS-card and calculated ones using Mathcad 14 software

Sample ID	**Lattice Parameter/Å (JCPDS-card)**	**Lattice Parameter/Å (Mathcad 14 software)**
LSCF (Orthorombic)	a = 5.475	a = 5.471
	b = 5.536	b = 5.482
	c = 7.848	c = 7.900
BCZY (Cubic)	a = 4.3436	a = 4.335

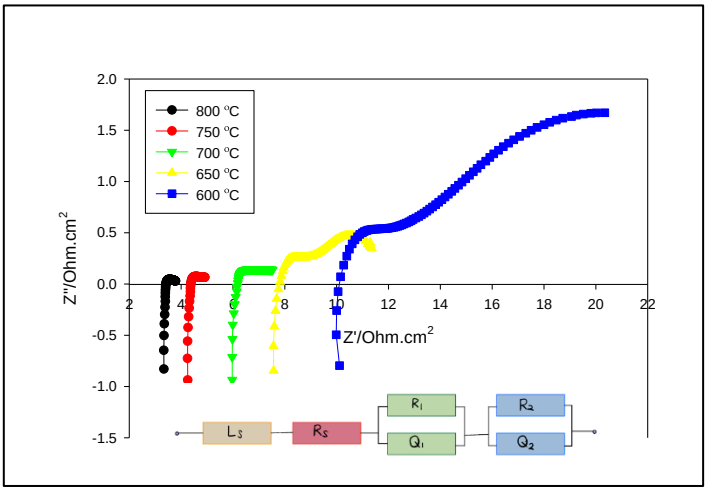

Figure 2. The EIS spectrum of LSCF-BCZY|BCZY|LSCF-BCZY under humidified air at the temperature in the range of 600 °C to 800 °C (Inset is the used equivalent circuit to resolve the associated responses)

Table 2. The calculated values of capacitance, arc summit frequencies and R_p and ASR for the LSCF-BCZY|BCZY|LSCF-BCZY

Temperature (°C)	**Capacitance, C (Fcm^2)**	**Arc summit frequency, f° (Hz)**	**Polarization Resistance, R_p (Ωcm^2)**	**Area specific resistance, ASR (Ωcm^2)**
800	C_1: 3.08x10^{-5}	$f°_1$: 1.09x10^4	R_1: 0.080	0.250
	C_2: 2.58x10^{-2}	$f°_2$: 2.67x10^3	R_2: 0.420	
			R_p: 0.500	
750	C_1: 2.39x10^{-5}	$f°_1$: 5.35x10^6	R_1: 0.075	0.332
	C_2: 7.86x10^{-1}	$f°_2$: 4.89x10^3	R_2: 0.589	
			R_p: 0.664	

Table 2 (cont'd). The calculated values of capacitance, arc summit frequencies and R_p and ASR for the LSCF-BCZY|BCZY|LSCF-BCZY

Temperature (°C)	Capacitance, C (Fcm^2)	Arc summit frequency, f° (Hz)	Polarization Resistance, R_p (Ωcm^2)	Area specific resistance, ASR (Ωcm^2)
700	C_1: 1.02x10^{-5} C_2: 2.40x10^{-1}	f°$_1$: 3.37x10^5 f°$_2$: 1.67x10^2	R_1: 0.750 R_2: 1.290 R_p: 2.040	1.020
650	C_1: 3.11x10^{-6} C_2: 1.79x10^{-2}	f°$_1$: 2.81x10^4 f°$_2$: 3.16x10^2	R_1: 0.800 R_2: 2.478 R_p: 3.278	1.639
600	C_1: 8.46x10^{-5} C_2: 1.79x10^{-2}	f°$_1$: 2.14x10^4 f°$_2$: 5.35x10^2	R_1: 2.100 R_2: 9.400 R_p: 11.500	5.750

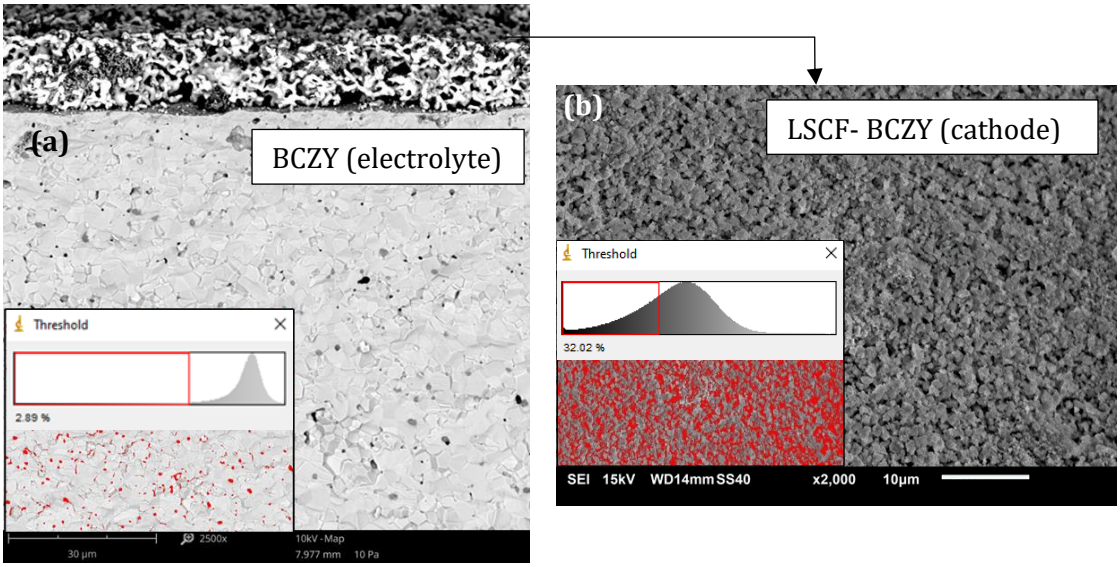

Figure 3. SEM images of the LSCF-BCZY|BCZY|LSCF-BCZY after electrochemical measurement (a) cross section and (b) top view of the cell

Conclusion

The LSCF and BCZY powders were prepared by the sol-gel method using metals nitrate salts. Both compounds maintained their respective phase even after they were simultaneously calcined at 900 °C. ASR values at the intermediate temperatures of 800 to 600 °C with the composite cathode half-cell were 0.25, 0.33, 1.02, 1.64, and 5.75 Ω.cm^2. After the electrochemical testing, the morphology of the well-distributed cells remained unchanged, i.e., with no delamination and porosity optimised. The use of the LSCF-BCZY composite cathode reduced the polarization resistance of the fabricated cell substantially, suggesting that it might have great potential for PCFC application.

Acknowledgement

We acknowledged Strategic Research Partnership Grant UiTM-UTM (100-RMC 5/3/SRP GOV(002/2021)) for the sponsorship and UiTM for the facilities.

References

1. He, W., Yuan, R. H., Dong, F. F., Wu, X. L. and Ni, M. (2017). High performance of protonic solid oxide fuel cell with $BaCo_{0.7}Fe_{0.22}Sc_{0.08}O_{3-\delta}$ electrode. *International Journal of Hydrogen Energy,* 42(39): 25021-25025.
2. Chen, J., Li, J., Jia, L., Moussa, I., Chi, B., Pu, J. and Li, J. (2019). A novel layered perovskite Nd $(Ba_{0.4}Sr_{0.4}Ca_{0.2})$ $Co_{1.6}Fe_{0.4}O_{5+\delta}$ as cathode for proton-conducting solid oxide fuel cells. *Journal of Power Sources,* 428: 13-19.
3. Fang, X., Zhu, J. and Lin, Z. (2018). Effects of electrode composition and thickness on the mechanical performance of a solid oxide fuel cell. *Energies,* 11(7): 1735.
4. Osman, N., Ismail, I., Samat, A. A. and Md Jani, A. M. (2016). Reactivity study of $LaSrCoFeO_3$-Ba (Ce, Zr) O_3 composite cathode material. *In Materials Science Forum,* 846: pp. 58-62.
5. Ismail, I., Osman, N. and Jani, A. M. M. (2018). Evaluation of $La_{0.6}Sr_{0.4}Co_{0.2}Fe_{0.8}O_{3-\delta}$ as a potential cathode for proton-conducting solid oxide fuel cell. *Sains Malaysiana,* 47(2): 387-391.
6. Matsui, T., Kunimoto, N., Manriki, K., Miyazaki, K., Kamiuchi, N., Muroyama, H. and Eguchi, K., 2021. Oxygen reduction reaction over (Ba, $Sr)_6RE_2Co_4O15$–$Ba(Ce,Pr,Y)O_3$ composite cathodes for proton-conducting ceramic fuel cells. *Journal of Materials Chemistry* A, 9(27): 15199 15206.
7. Loureiro, F. J., Ramasamy, D., Mikhalev, S. M., Shaula, A. L., Macedo, D. A. and Fagg, D. P. (2021). $La_4Ni_3O_{10}$±δ–$BaCe0.9Y0.1O_3$-δ cathodes f or proton ceramic fuel cells; short-circuiting analys is using BaCe0. 9Y0. 1O3-δ symmetric cells. *International Journal of Hydrogen Energy*, 46(25): 13594-13605.
8. Song, Y., Chen, Y., Wang, W., Zhou, C., Zhong, Y ., Yang, G., ... and Shao, Z. (2019). Self-assembled triple-conducting nanocomposite as a superior protonic ceramic fuel cell cathode. *Joule*, *3*(11): 28 42-2853.
9. Shao, L., Si, F., Fu, X. Z. and Luo, J. L. (2018). Stable $SrCo0.7Fe0.2Zr0.1O_3$-δ cathode material for proton conducting solid oxide fuel cell reactors. *International Journal of Hydrogen Energy*, *43*(15): 7511-7514.
10. Zhu, H., Ricote, S., Duan, C., O'Hayre, R. P., Tsvetkov, D. S. and Kee, R. J. (2018). Defect incorporation and transport within dense $BaZr_{0.8}Y_{0.2}O_{3-\delta}$ (BZY_{20}) proton-conducting membranes. *Journal of The Electrochemical Society,* 165(9): F581.
11. Osman, N., Senari, S. M. and Md Jani, A. M. (2020). Characterization of NiO-BCZY as composite anode prepared by a one-step sol-gel method. *Malaysian Journal of Fundamental and Applied Sciences,* 16(4): 450–452.
12. Miao, L., Hou, J., Gong, Z., Jin, Z. and Liu, W. (2019). A high-performance cobalt-free Ruddlesden-Popper phase cathode $La_{1.2}Sr_{0.8}Ni_{0.6}Fe_{0.4}O_{4+\delta}$ for low temperature proton-conducting solid oxide fuel cells. *International Journal of Hydrogen Energy,* 44(14): 7531-7537.
13. Mohsin, M., Yousaf, A., Raza, R. and Zia, R. (2019). Highly conducting perovskite structured (M-$SrCoFe-O_{3-\delta}$, M= Ce, Ba) cathode for solid oxide fuel cell. *Journal of Alloys and Compounds,* 791: 248-254.
14. Lee, S., Park, S., Wee, S., woo Baek, H. and Shin, D. (2018). One-dimensional structured $La_{0.6}Sr_{0.4}Co_{0.2}Fe_{0.8}O_{3-\delta}$-$BaCe_{0.5}Zr_{0.35}Y_{0.15}O_{3-\delta}$ composite cathode for protonic ceramic fuel cells. *Solid State Ionics,* 320: 347-352.
15. Osman, N., Ismail, I., Samat, A. A. and Md Jani, A. M. (2016). Reactivity study of $LaSrCoFeO_3$-Ba (Ce, Zr)O_3 composite cathode material. *In Materials Science Forum,* 486: 58-62.
16. Kuroha, T., Yamauchi, K., Mikami, Y., Tsuji, Y., Niina, Y., Shudo, M., ... and Okuyama, Y. (2020). Effect of added Ni on defect structure and proton transport properties of indium-doped barium zirconate. *International Journal of Hydrogen Energy,* 45(4): 3123-3131.
17. Baek, S.-W., J. Bae, and Y.-S. Yoo, Cathode reaction mechanism of porous-structured $Sm0.5Sr0.5CoO_3$−δ and $Sm0.5Sr0.5CoO_3$−δ/ Sm0.2Ce0.8O1.9 for solid oxide fuel cells. *Journal of Power Sources,*193(2): 431-440.